Journal of The Electrochemical Society

The Electrochemical Society
Advancing solid state & electrochemical science & technology

OPEN ACCESS

# Passivation of Cu-Rh Alloys

To cite this article: Yusi Xie *et al* 2021 *J. Electrochem. Soc.* **168** 071505

*Journal of The Electrochemical Society*, 2021 **168** 071505

# Passivation of Cu-Rh Alloys

**Yusi Xie,[1] Swarnendu Chatterjee,[1] Ling-Zhi Liu,[2] Hai-Jun Jin,[2] and Karl Sieradzki[1,z]**

[1]*Ira A. Fulton School of Engineering, Arizona State University, Tempe, Arizona 85287, United States of America*
[2]*Shenyang National Laboratory for Materials Science, Institute of Metal Research, Chinese Academy of Sciences, Shenyang 110016, People's Republic of China*

Historically, there have been two general approaches for understanding alloy passivation behavior. One involves study of the composition and crystal structure of the passive film and the other is concerned with how the composition and structure of the metallic alloy dictates the formation of the film. Herein we describe a recently developed theory based on a conjecture of Sieradzki and Newman connected to percolation theory and use the theory to model the passivation behavior of a series of Cu-Rh alloys. Our results are in quantitative agreement with the predictions of this theory. We discuss how the theory elucidates the important role of short-range order in understanding how composition affects the details of the passivation process.

 [DOI: 10.1149/1945-7111/ac0f60]

Manuscript submitted June 4, 2021; revised manuscript received June 24, 2021. Published July 7, 2021.

Alloy design against aqueous corrosion involves an understanding of the detailed atomic-scale processes responsible for passivation. Thermodynamics on its own is of limited use as passive films represent structures that can be far from equilibrium. Fe-Cr alloys which have historically served as the prototypical system for the study of passivation[1–11] is an example of this, as the potential-pH diagram of elemental Cr provides us with no hint that this metal passivates in acid electrolytes.[12] Passivation of Fe-Cr alloys, stainless steels, Ni-Cr alloys and numerous other alloy systems has been studied by examining the composition and crystal structure of the nanometer-scale protective oxide.[13] Importantly, such characterization studies have not contributed much useful information on the initial stages of the passivation process which occurs within time scales of order seconds or less[14] and likely involves an initially amorphous oxide structure that gradually crystallizes over times scales of minutes to hours,[9,10] finally resulting in passive current densities of order 1 $\mu$A cm$^{-2}$.

Recently, we developed a quantitative atomic-scale theory of the passivation process that can be used in the design of new families of alloys such as the so-called multi-principle element alloys (MPEAs).[15] The basics of this theory are as follows. The starting point of our theory is a conjecture by Sieradzki and Newman that identified site percolation as an important process in alloy passivation.[16] At that time, it was envisioned that the initial stage of passive film formation on Fe-Cr alloys involves a competition between nucleation of nanometer-scale, spatially localized incipient oxide nuclei (*here termed Cr-O-Cr- mer-units*) and the selective dissolution of Fe, which as shown in Fig. 1, can undercut these mer-units and detach them from the alloy surface. It was reasoned that the only way of preventing undercutting was by some kind of mer-unit percolation phenomenon. One important physical length scale immediately apparent from this conjecture is the Cr-Cr separation distance within the bulk of the alloy, since oxygen has to be able to bridge these sites in order to form mer-units. This separation distance sets the minimum mole fraction of Cr in the lattice that allows for the development of percolating mer-units, as determined by the alloy crystal structure and lattice parameter. For a perfectly random solid solution alloy, this distance is given by, $p_c^{3D}\{n_i\}$, where, $p_c^{3D}\{n_i\}$ is the 1st ($i = 1$), 1st + 2nd ($i = 2$) or the 1st + 2nd + 3rd ($i = 3$) nearest neighbor (NN) 3D site percolation thresholds. The body-centered cubic thresholds are $p_c^{3D}\{n_1\} = 0.243$, $p_c^{3D}\{n_2\} = 0.175$, *and* $p_c^{3D}\{n_3\} = 0.095$.[17] Well-known ionic radii data[18] were used to determine the spanning distance required for mer-unit formation. Since in the BCC Fe-Cr lattice, separation between 3rd NN allows for mer-unit formation, the minimum required "critical" mole fraction of Cr was reasoned to be 0.095.[16]

At the time of the Sieradzki and Newman conjecture, there were two additional critical components missing from the model. One is connected to the fact that no real alloys of interest correspond to ideal solid solutions or perfect mixing of the components.[19] All real single-phase alloys have some degree of short-range order (SRO) as characterized by, for example, the well-known Warren-Cowley (WC) SRO parameter.[20,21] SRO can significantly attenuate the percolation thresholds defined above.[15] The other key missing ingredient to the theory is connected to selective dissolution which often precedes the passivation process. Selective dissolution will allow for percolation across the two-dimensional (2D) roughened topological surface at Cr compositions below conventional 2D site percolation thresholds.[15] A simple analogy is connected to the electrical conductivity of a randomly mixed composite material composed of electrically conducting and non-conductive elements.[22] Figure 2 shows a cross-section of such a composite composed of cubic elements at a composition above the three dimensional 1st NN site percolation threshold for the cubic lattice ($p_c^{3D}\{n_1\} = 0.30$) but below the 2D site percolation threshold of the square lattice ($p_c^{2D}\{n_1\} = 0.59$). As a result of NN connectivity in the thickness direction, the conducting surface elements shown in Fig. 2 are electrically connected. The thickness, $h$, over which connectivity occurs is a function of the fraction of conducting elements in the composite. Now imagine that the white colored elements correspond to Fe atoms that are selectively dissolved resulting in a roughened 2D surface with increased Cr atom fraction. Cr now percolates across the roughened topological surface. The relationship between the thickness, $h$, and the atom fraction of Cr in the alloy required for this transitional percolation behavior is given by, $h = c[p_c(h) - p_c^{3D}\{n_i\}]^{-\nu_{3D}}$[15,23] Here $c$ is a constant of order unity, $\nu_{3D}$ is a percolation scaling exponent which has a universal value of 0.878 in 3D, $p_c^{3D}\{n_i\}$ is the relevant site percolation threshold in the thermodynamic limit (e.g., the values quoted above for random mixing in a BCC lattice for $h = \infty$) and $p_c(h)$ is a series of $h$-dependent, 2D percolation thresholds on the topologically roughened surface, determined by the alloy composition.[15,23] In an experiment, $h$ represents the number of layers that have to dissolve in order for Cr to percolate across the corrosion roughened surface. The key length scales emerging from the theory are the Cr atom spacing in the lattice required to form the mer-units and $h$. In general, both of these parameters will depend on the SRO in the alloy.

Our previous work examined the passivation behaviors of Fe-Cr and Ni-Cr alloys within the context of the theory described above.[15] In pursuit of extending the model to non-Fe- and Ni-base alloys,

[z]E-mail: Karl.Sieradzki@asu.edu

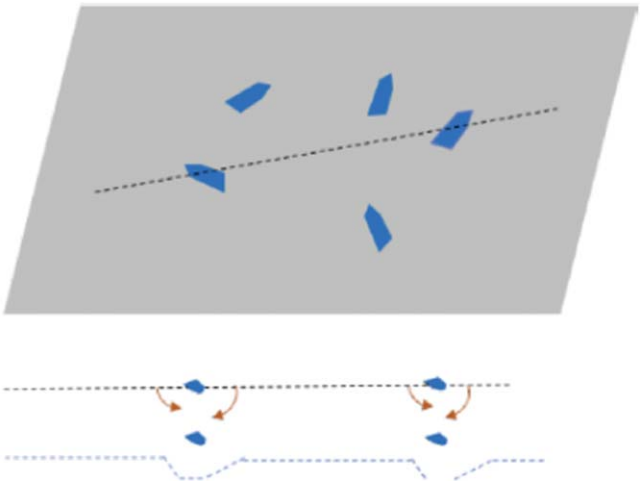

**Figure 1.** Cartoon illustrating undercutting of non-percolating Cr-O-Cr mer-units in binary Fe-Cr alloys. These mer-units or incipient Cr-rich oxide clusters (blue) which are less than 1 nm in size are embedded in the first metal monolayer. Selective Fe dissolution (brown arrows) results in the formation of "pits" several monolayers deep and the detachment of the mer-units from the surface.

herein, we report on the behavior of Cu-Rh alloys. This is a particularly interesting alloy system since the selective dissolution of Cu can result in the formation of nanoporous Rh and depending on the alloy composition, clear active to passive waves are present in the linear sweep voltammetry of these alloys.[24] The Cu-Rh phase diagram shows that within a range of temperature and composition, a single-phase, face-centered cubic (FCC) crystal structure is thermodynamically stable[25]. At temperatures below about 500 °C, the system tends to cluster and phase separate.

## Experimental Methods

Cu-Rh alloys with Rh mole fractions of 0.07, 0.10, 0.13, 0.16, 0.18, 0.20, 0.22 were prepared by arc melting Cu wires (99.999%) and Rh sheets of (99.95%) at the indicated purities, under an argon atmosphere. These samples were homogenized at 1000 °C for one week and quenched in water. The compositions and homogeneity of the samples was confirmed by energy dispersive spectroscopy. Cylindrical disk samples (5 mm in diameter and 5 mm in height) were fabricated by electro-discharge machining. Sample surfaces were mechanically polished to 1 $\mu$m diamond paste and cleaned prior to each electrochemical experiment. Linear sweep voltammetry (LSV) at a ramp rate 5 $mVs^{-1}$ and chronoamperometry were performed in de-aerated 0.1 M $H_2SO_4$ immediately following

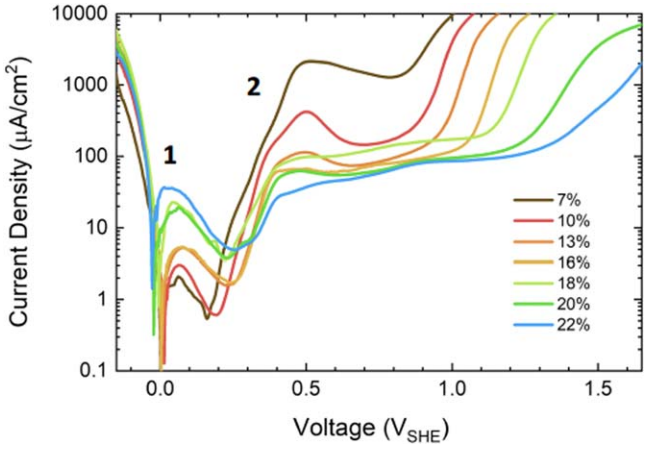


**Figure 3.** LSV of Cu-Rh alloys at the indicated compositions. The H oxidation wave is labeled 1 and the passivation wave is labeled 2.

reduction of the air formed film. The air-formed oxide was cathodically reduced at −0.2 V (SHE) for 100 s. Fresh electrolyte was used for each experiment. Ultra-high purity nitrogen gas was used to de-aerate the solution and a flow of this gas was maintained over the surface of the electrolyte following de-aeration for the duration of each experiment. Chronoamperometry data related to the passivation process were collected within the initial 400 s after a voltage pulse from 0.160 −260 V (depending on alloy composition) to 0.640 V (SHE) which was based on the LSV behavior. Platinum mesh and a mercury-mercurous sulfate electrode (MSE) were used as the counter electrode and reference electrode, respectively. All potentials are reported relative to standard hydrogen electrode (SHE).

## Results

Figure 3 shows the LSV data obtained on the Cu-Rh alloys at Rh mole fractions ranging from 0.07 to 0.220. The first wave occurring at c. a. 0.0 V (SHE) is related hydrogen (H) desorption/oxidation as a result of the air-formed film reduction protocol used. Chronocoulometry (voltage pulse from −0.200 V to the minimum in the wave as determined from the LSV) was used to assess the quantity of absorbed H. To our knowledge, H does not underpotentially deposit or absorb into elemental Cu, while it is known to underpotentially deposit on elemental Rh electrodes.[26,27] There are also reports that Rh and Ag-Rh nanoparticles are able to store hydrogen.[28,29] Therefore, we attribute this wave to the Rh component in the alloy. Figure 4 shows the result of this hydrogen oxidation analysis. The charge density increases exponentially with the mole fraction of Rh

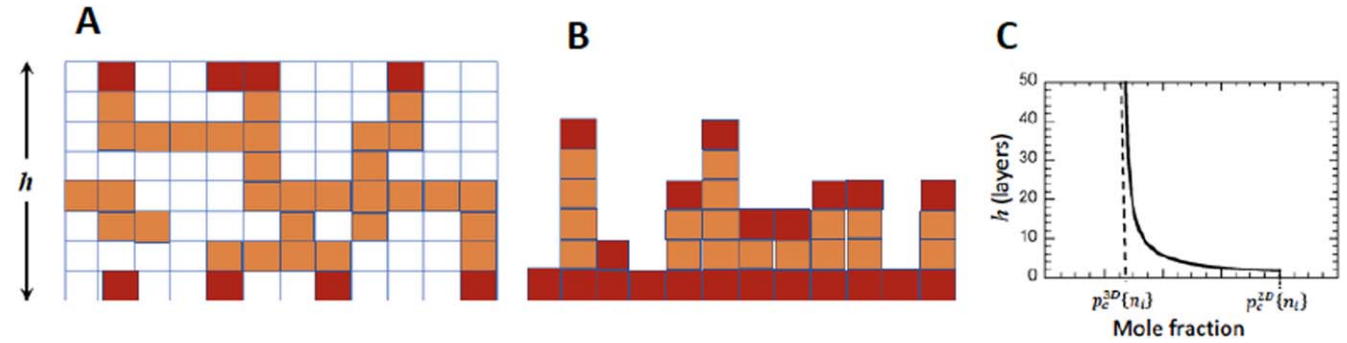


**Figure 2.** Composite conductivity analogy and alloy passivation. (A) Cross-section of a composite with electrically conductive elements on the surface (red), in the bulk (orange) and non-conductive elements (white). A two-point resistivity measurement placed on any of the red elements would show that they are electrically connected even though this is not apparent by examining the surface. (B) If the white elements are now considered to be Fe and the red/orange elements, Cr, selective dissolution of Fe results in a Cr structure that percolates across the surfaces. (C) Qualitative plot showing the theoretical behavior of the number of layers dissolved required for 2D percolation across the topologically roughened or corroded surface as a function of the Cr composition, $p$. The $x$-axis defines a series of $h$-dependent 2D percolation thresholds.

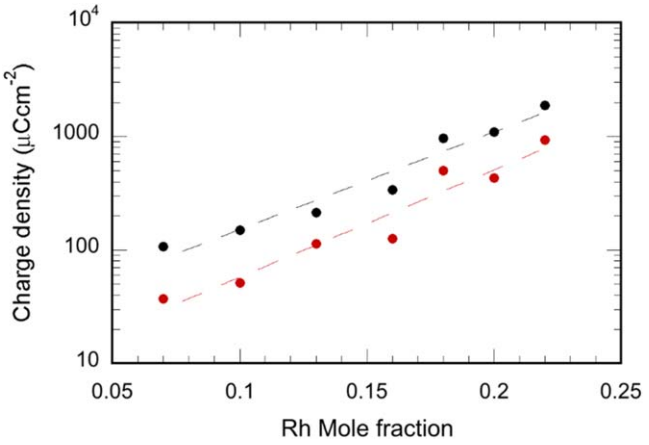


**Figure 4.** Charge density associated with the H oxidation as a function of Rh mole fraction. Red points integrated from the LSV; black points chronoamperometry. The dashed lines serve as a guide to the eye.

in the alloy. This behavior is consistent with predictions of percolation theory for Rh compositions not too close to the percolation threshold. The FCC 1st NN site percolation threshold is 0.195.[17] Below this threshold, only finite-sized ramified or fractal Rh clusters are connected to the electrode surface and above the threshold the clusters become more compact or droplet shaped.[30] Assuming that the hydrogen only adsorbs at the interface of Rh clusters and the Cu component, we would expect a maximum in adsorption at the percolation threshold, where ramification (in the sense of surface to volume ratio) of the "infinite" cluster is greatest.[30] Given that we only examined the behavior of alloys containing up to 22 at% Rh, we cannot further assess the hydrogen behavior. However, it seems possible that such measurements may be used to determine the percolation threshold in this alloy (by determining the composition associated with the maximum in charge density) which may be different than the conventional ideal solid solution value of 0.195, as a result of short-range order effects.[15]

At potentials larger than about 0.22 V, selective dissolution of Cu occurs and the corroded alloy surface is enriching in Rh. Subsequently, we observe a wave associated with an active/passive transition. The peak position and detailed structure of these waves are dependent on alloy composition. Figure 5 shows the results of potential-pulse, chronoamperometry experiments conducted from ~0.220 (depending on alloy composition) to 0.640 V. The lower voltage limit corresponds to the decay of the H-related wave and the upper limit corresponds to completion of the compositional dependent passivation waves. The charge density associated with the base-line (passive current density at 400 s) subtracted chronoamperometry data was converted to the number of dissolved layers corresponding to $h$ in the model using,[15]

$$h = \frac{\int_0^t I\,dt}{A} \Bigg/ \frac{4 * (3 * p + 2 * (1 - p)) * q}{\sqrt{3} * a_{Cu}^2}$$

where $A$ is exposed surface area, $I$ is the magnitude of time-dependent current, $p$ is the mole fraction of Rh, $q$ is the elementary charge, and $a_{Cu}$ is the lattice parameter of FCC Cu. This calculation was performed assuming that Cu dissolved as $Cu^{2+}$, Rh was oxidized to $Rh^{3+}$ (in the mer-unit) and that the surface orientation of the electrodes was (111).

## Discussion

Figure 3 shows that the active to passive transition for the Cu-Rh alloy compositions examined, occurs near 500 mV SHE, while the conventional Pourbaix diagram for elemental Rh predicts that oxidation will occur at 740 mV SCE.[12] However, Capon and Parsons have shown that in 1 M $H_2SO_4$, Rh oxidation initiates at a potential of 440 mV SCE.[26] Additionally, Hourani and Wieckowski showed that in 1 M $HClO_4$, Rh oxidation initiates at about 430 mV SCE.[27] Ancillary LSV results obtained in our own laboratory show that in 0.1 M $H_2SO_4$, and at a sweep rate of 5 $mVs^{-1}$, Rh oxidation/passivation initiates close to 500 mV SCE, which, other than slight variations resulting from alloying,[15] is quite close to the occurrence of the active/passive transition observed for the Cu-Rh alloys.

The face-centered cubic thresholds for a random solid solution are $p_c^{3D}\{n_1\} = 0.195$, $p_c^{3D}\{n_2\} = 0.136$, *and* $p_c^{3D}\{n_3\} = 0.061$.[17] The neighbor distances and the Rh-O-Rh spanning distance as a function of composition are shown in Fig. 6. Figure 7 shows the fit to the theory based on the chronoamperometry yielding a $p_c^{3D}\{n_i\} = 0.062$. Binary alloy systems that show a tendency toward ordering in the first nearest neighbor shell (negative WC SRO parameter) tend to show a tendency toward clustering (positive WC SRO parameter) in the second nearest neighbor shell.[20,21,31–34] Our previous work for the BCC Fe-Cr system showed that if an alloy has a tendency toward NN clustering, conventional percolation thresholds are reduced and a tendency for ordering results in an increase.[15,35] Based on this, we would predict that the $p_c^{3D}\{n_1\}$ value in the Cu-Rh alloy is increased from its conventional value of 0.195 and that $p_c^{3D}\{n_2\}$ is decreased from 0.136. This prediction of ordering in the first NN shell for Cu-Rh alloys can be tested using X-ray absorption fine structure (XAFS),[36] neutron scattering[34] or Mössbauer spectroscopy.[31–33]

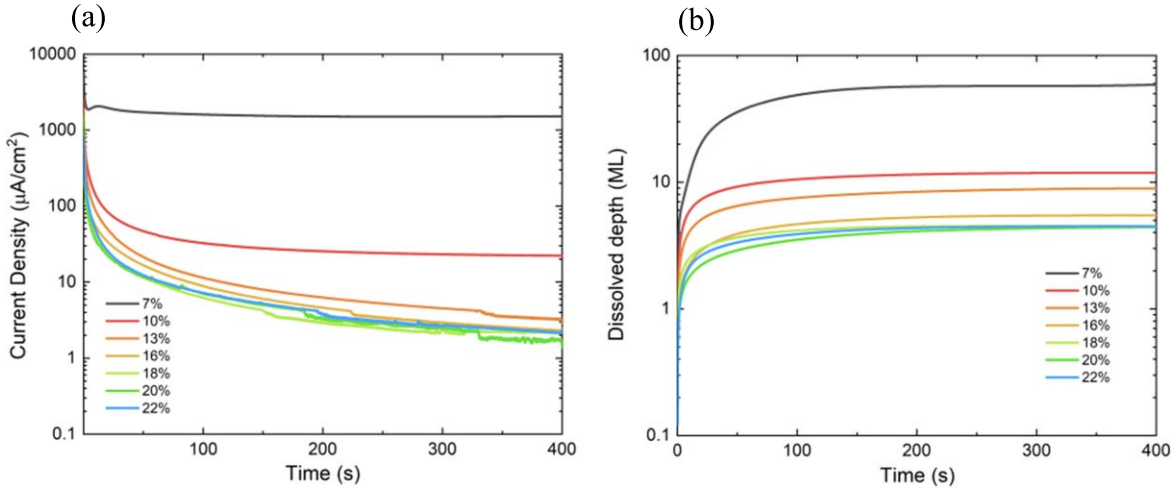


**Figure 5.** Chronoamperometry at 0.640 V. (A) Current density as a function of time and (B) number of layers dissolved as a function of time.

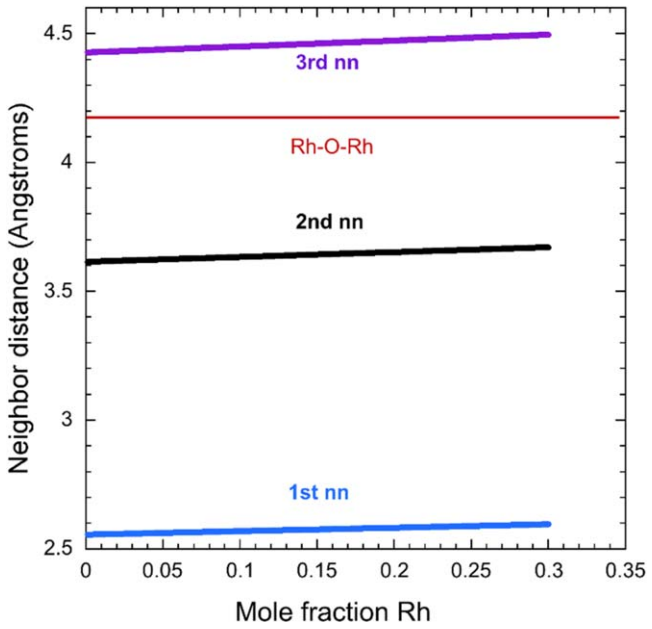


**Figure 6.** Length scales in the Cu-Rh lattice compared to the Rh-O-Rh mer spanning length. The Rh-O-Rh spanning length fall between 2nd and 3rd NN distances in the FCC Cu-Rh lattice.

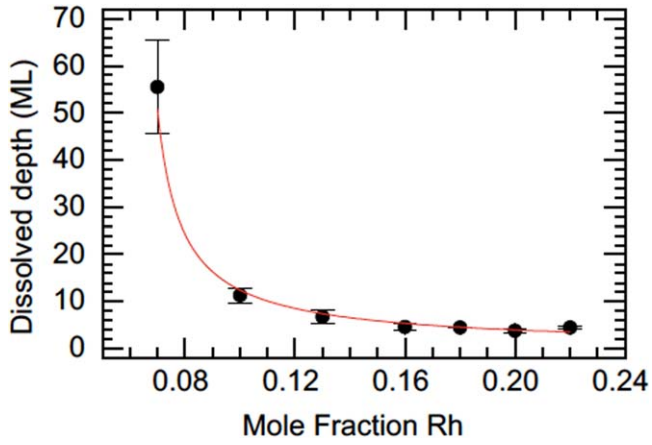


**Figure 7.** $h$ vs mole fraction of Rh in Cu-Rh alloys. The red curve shows the fit to the theoretical equation, $h = 0.698[p_c(h) - 0.062]^{-0.878}$. The error bars represent the standard deviation n tihree data sets.

Extending our model to other families of alloys such as refractories requires the use of an experimental characterization technique capable sorting out selective dissolution processes from solid-state oxidation, since many refractory elements display multiple oxidation states. One such characterization technique is on-line inductively coupled plasma mass spectroscopy.[37,38] The online component is necessary since it is important to be able correlate time-dependent measured currents in LSV or potential-dependent chronoamperometry to the identity and mass of elemental components dissolving from the alloy.

Finally, we would like to take this opportunity to comment on the important contribution that first-principles based calculations can make to the understanding of alloy passivation. Consider an alloy at a composition $A_pB_{1-p}$ where p is the mole fraction of the passivating component, A. We can take the B "component" to be a single element, such as Cu in the system reported on herein, or even a combination of elements such as that in a MPEA. As a function of p, the atomic-scale distribution of the A cluster size dictates the ability of this component to form incipient oxide mer-units.[15] How do the populations of A monomers, dimers, trimers, etc affect the electrochemical potential for mer-unit formation? Clearly knowledge of SRO in alloys of interest are expected to have a large effect on the compositionally dependent A-cluster populations.

## Conclusions

Cu-Rh alloys show passivation behavior in excellent quantitative agreement with the percolation theory of alloy passivation. Based on both the H oxidation behavior and the passivation behavior, the theory predicts that for the heat-treatments used, these alloys will show a tendency toward ordering in the 1st nearest neighbor shell and clustering in the 2nd nearest neighbor shell. Future high fidelity XAFS research on Cu-Rh alloys is planned which should serve as a further test of the theory.

## Acknowledgments

YX, SC and KS acknowledge funding from the National Science Foundation under award DMR-1708459. HJJ and LZL acknowledge funding from the National Natural Science Foundation of China under Grant No. 51971218.

## ORCID

Karl Sieradzki https://orcid.org/0000-0002-4789-3956

## References

1. H. H. Uhlig and G. E. Woodside, "Anodic polarization of passive and non-passive chromium–iron alloys." *J. Phys. Chem.*, **57**, 280 (1953).
2. P. F. King and H. H. Uhlig, "Passivity in the iron-chromium binary alloys." *J. Phys. Chem.*, **63**, 2026 (1959).
3. R. P. Frankenthal, "On the passivity of iron-chromium alloys i. reversible primary passivation and secondary film formation." *J. Electrochem. Soc.*, **114**, 542 (1967).
4. R. P. Frankenthal, "On the passivity of iron-chromium alloys ii. the activation potential." *J. Electrochem. Soc.*, **116**, 580 (1969).
5. R. P. Frankenthal, "On the passivity of iron-chromium alloys III. effect of potential." *J. Electrochem. Soc.*, **116**, 1646 (1969).
6. M. Keddam, O. R. Mattos, and H. Takenouti, "Mechanism of anodic dissolution of iron-chromium alloys investigated by electrode impedances-I. experimental results and reaction model." *Electrochim. Acta*, **31**, 1147 (1986).
7. M. Keddam, O. R. Mattos, and H. Takenouti, "Mechanism of anodic dissolution of iron-chromium alloys investigated by electrode impedances-II. elaboration of the reaction model." *Electrochim. Acta*, **31**, 1159 (1986).
8. R. Kirchheim, B. Heine, H. Fischmeister, S. Hofmann, H. Knote, and U. Stolz, "The passivity of iron-chromium alloys." *Corros. Sci.*, **29**, 899 (1989).
9. M. P. Ryan, R. C. Newman, and G. E. Thompson, "A scanning tunneling microscopy study of structure and structural relaxation in passive oxide films on Fe-cr alloys." *Philos. Mag. B*, **70**, 241 (1994).
10. M. P. Ryan, R. C. Newman, and G. E. Thompson, "Atomically resolved STM of oxide film structures on Fe-Cr alloys during passivation in sulfuric acid solution." *J. Electrochem. Soc.*, **141**, L164 (1994).
11. A. J. Davenport, M. P. Ryan, M. C. Simmonds, P. Ernst, R. C. Newman, S. R. Sutton, and J. S. Colligon, "In Situ synchrotron X-ray microprobe studies of passivation thresholds in Fe-Cr alloys." *J. Electrochem. Soc.*, **148**, B217 (2001).
12. M. Pourbaix, *Atlas of Electrochemical Equilibria in Aqueous Solution* (National Association of Corrosion Engineers (NACE), Houston, Texas) 2nd ed. (1974).
13. P. Marcus and I. Olefjord, "Round robin on combined electrochemical and AES/ESCA characterization of the passive films on Fe-Cr and Fe-Cr-Mo alloys." *Surf. Interface Anal.*, **11**, 569 (1988).
14. P. D. Bastek, R. C. Newman, and R. G. Kelly, "Measurement of passive film effects on scratched electrode behavior." *J. Electrochem. Soc.*, **140**, 1884 (1993).
15. Y. Xie et al., "A percolation theory for designing corrosion resistant alloys." *Nat. Mater.*, **20**, 789 (2021).
16. K. Sieradzki and R. C. Newman, "A percolation model for passivation in stainless steels." *J. Electrochem. Soc.*, **133**, 1979 (1985).
17. V. K. S. Shante and S. Kirkpatrick, "An introduction to percolation theory." *Adv. Phys.*, **20**, 325 (1971).
18. R. D. R. Shannon, "Effective ionic radii and systematic studies of interatomic distances in halides and chalcogenides." *Acta Cryst., A*, **32**, 751 (1976).
19. G. R. Gaskell, *Introduction to the Thermodynamics of Materials* (Taylor & Francis, New York, NY) 4th ed. (2003).
20. J. M. Cowley, "An approximate theory for order in alloys." *Phys. Rev.*, **77**, 669 (1950).
21. J. M. S.-R. Cowley, "Order and long-range order parameters." *Phys. Rev.*, **A138**, 1384 (1965).
22. J. P. Clerc, G. Giraud, S. Alexander, and E. Guyon, "Conductivity of a mixture of conducting and insulating grains: dimensionality effects." *Phys. Rev. B*, **22**, 2489 (1980).
23. P. Sotta and D. Long, "The crossover from 2D to 3D percolation: theory and numerical simulations." *Eur. Phys. J. E*, **11**, 375 (2003).

24. F. Liu and H.-J. Hin, "Extrinsic parting limit for dealloying of Cu-Rh." *J. Electrochem. Soc.*, **140**, C999 (2018).
25. ASM Handbook, *Alloy Phase Diagrams*, ed. H. Baker (ASM Intertnational,, Metals Park, Ohio) 3 (1992).
26. A. Capon and R. Parsons, "The effect of strong acid on the reactions of hydrogen and oxygen on the noble metals. A study using cyclic voltammtery and a new teflon electrode holder." *Electroanal. Chem.*, **39**, 275 (1972).
27. M. Hourani and A. Wieckowski, "Single crystal electrochemistry of rhodium. Anion effects and order/disorder transitions of clean and silver coated Rh (111) surfaces." *J. Electroanal. Chem.*, **244**, 147 (1988).
28. H. Kobayashi, H. Morita, M. Yamauchi, R. Ikeda, H. Kitagawa, Y. Kubota, K. Kato, and M. Takata, "Nanosize-induced hydrogen storage and capacity control in a non-hydride-forming element: rhodium." *J. Am. Chem. Soc.*, **133**, 11034 (2011).
29. K. Kusada, M. Yamauchi, H. Kobayashi, H. Kitagawa, and Y. Kubota, "Hydrogen-storage properties of solid-solution alloys of immiscible neighboring elements with Pd." *J. Am. Chem. Soc.*, **132**, 15896 (2010).
30. D. Stauffer and A. Aharony, *Introduction to Percolation Theory* (Taylor & Francis, Philadelphia, PA) 2nd ed. (1994).
31. S. M. Dubiel and J. Cieślak, "Effect of thermal treatment on the short-range order in Fe–Cr alloys." *Mater. Lett.*, **107**, 86 (2013).
32. S. M. Dubiel, J. Cieślak, and J. Zukrowski, "Distribution of Cr atoms in the surface zone of Fe-rich Fe–Cr alloys quenched into various media: mössbauer spectroscopic study." *Appl. Surf. Sci.*, **359**, 526 (2015).
33. S. M. Dubiel and J. Cieslak, "Short-range order in iron-rich Fe-Cr alloys as revealed by mössbauer spectroscopy." *Phys. Rev. B*, **83**, 180202 (2011).
34. I. Mirebeau and G. Parette, "Neutron study of the short range order inversion in $Fe_{1-x}Cr_x$." *Phys. Rev. B*, **82**, 104203 (2010).
35. M. Liu, A. Aiello, Y. Xie, and K. Sieradzki, "The effect of short-range order on passivation of Fe-Cr alloys." *J. Electrochem. Soc.*, **165**, C380 (2018).
36. B. Ravel and M. A. T. H. E. N. A. Newville, "Artemis, Hephaestus: data analysis for X-ray absorption spectroscopy using IFEFFIT." *J. Synchrotron Radiat.*, **12**, 537 (2005).
37. P. P. Lopes, D. Strmcnik, D. Tripcovik, J. G. Connell, V. Stamenkovic, and N. M. Markovic, "Relationships between Atomic Level Surface Structure and Stability." *ACS Catal.*, **6**, 2536 (2016).
38. Y. Liu et al., "Stability limits and defect dynamics in Ag nanoparticles probed by bragg coherent diffractive imaging." *Nano Lett.*, **17**, 1595 (2017).